forum acusticum 2026
8-12 September · Graz, Austria

WINDOW GLAZING SYSTEMS DESIGN FOR INDOOR DRONE NOISE MITIGATION

Marco Oliveira[1], John Kennedy[2]

[1,2] *Faculty of Science, Technology, Engineering and Mathematics, Trinity College Dublin, Ireland*

This paper is a revised version of the authors` submitted manuscript that was peer-reviewed by at least two anonymous reviewers.

Abstract

Ensuring acoustic comfort is a key objective in building envelope design. In this context, common glazing systems are typically the weakest façade element, exhibiting sound insulation dips at the critical frequency (f_c) for monolithic glass and at the mass–air–mass resonance (f_0) for double-glazed units. Meanwhile, the dominant spectrum of drones (100–2500 Hz), including tonal peaks such as the blade-passing frequency, overlaps with these resonances and can readily transmit indoors. Therefore, this study evaluates the effectiveness of window glazing systems in mitigating indoor noise from drones. The sound insulation of various glazing configurations was analyzed in relation to the acoustic emissions of an octocopter delivery drone (2.5 kg payload). Results indicate that, among single-glazed systems 4–8 mm thick, laminated glazing outperforms annealed and tempered glass, achieving reductions of 4.2 dB(A) at f_c and up to 6.0 dB(A) in the 50-100 Hz range. For double-glazed systems, increasing the air gap from 12 mm to 50, 100, or 150 mm, combined with thicker glass, shifts f_0 to lower frequencies (48-97 Hz), resulting in improved low-frequency attenuation compared with conventional windows. The presented framework provides performance-based guidance for window design aimed at reducing drone noise in new residential buildings.

Keywords: *Drone Noise Mitigation, Façade Sound Insulation, Building Design, Window Glazing Systems*

1. Introduction

In recent years, research has increasingly focused on enhancing indoor comfort in buildings, with acoustic quality being recognized as a key contributing factor [1]. Within building design, façade sound insulation is crucial, as glazing systems often represent the limiting acoustic element when compared to opaque components [2]. Therefore, acoustic comfort depends on the appropriate selection of the glazing system and a thorough understanding of the external noise source, including its overall level and spectral characteristics. The performance of glazing systems is determined by their configuration and by several parameters, such as surface mass and stiffness of each pane, asymmetrical thicknesses to decouple resonant modes, cavity depth and gas filling, frame rigidity to minimize flanking transmission, and overall airtightness to prevent sound leakage. At the critical frequency (f_c), transmission loss experiences a marked dip, typically on the order of 8 to 10 dB, due to the coincidence effect [3]. This drop is particularly relevant when mitigating drone noise, as it implies that, for single-glazed systems, the primary strategy should be to shift f_c away from the dominant spectral content of the drone's acoustic signature. In double-glazed configurations, the most significant insulation deficit occurs at the mass–air–mass resonance frequency (f_0), at which the two panes are most strongly coupled [3]. Therefore, to ensure effective attenuation, f_0 must be tuned to lie below the drone's main frequency range. Although cavity resonances in the mid-to-high frequency range can also affect performance, they are not addressed in the present study, as f_0 exerts a considerably greater influence on the overall transmission loss. While the electrification of road transport may reduce traffic noise in cities [4], the emergence of advanced air mobility (AAM), encompassing drones and eVTOLs [5,6], introduces a new and spectrally distinct acoustic burden on buildings. The acoustic signature of a drone results from the interplay of design characteristics (dimensions, propulsion system, rotor geometry), operational state (payload, maneuvers, rotor speed), and environmental conditions (wind gusts) [6]. Delivery drones operate at altitudes between 50 and 120 m, placing them within the urban canopy layer, where atmospheric absorption is diminished. Few studies have specifically examined the impact of AAM on the built environment. Lee et

Corresponding author: *madeoliv@tcd.ie*

al. [7] employed numerical simulations to assess eVTOL noise around vertiports in South Korea, finding that while the equivalent level (L_{eq}) remains below 55 dB(A), the maximum level (L_{max}) inside nearby apartments can reach 55 dB(A). Ramos-Romero et al. [8] developed a methodology that integrates outdoor sound propagation with façade transmission loss to determine minimum operational distances for drones. Meanwhile, Masullo et al. [9] characterized noise emissions of small and medium-sized drones across different flight maneuvers at two receiver positions (ground and inside a building), showing that the small drone caused greater annoyance due to the stronger perceptual impact of its tonal components. Despite these valuable efforts, a critical research gap remains: How can different glazing systems effectively mitigate drone noise while ensuring compliance with indoor acoustic comfort recommendations? This work aims to address this gap by proposing an integrated methodology for glazing selection that balances drone noise attenuation with established indoor criteria. The remainder of this paper is organized as follows: Section 2 (Methodology); Section 3 (Results and Discussion); and Section 4 (Conclusions).

2. Methodology

This study employs a four-step sequential approach, beginning with the characterization of a delivery drone, and followed by the modeling of its acoustic propagation through an urban environment to a building façade. Subsequently, the acoustic performance of various glazing systems is evaluated against the drone's acoustic signature. Finally, these datasets are integrated to predict the resulting indoor noise levels within a bedroom of a representative residential building. Each step is detailed in the following subsections.

2.1 Drone Noise Data

The drone noise data was obtained from an experimental campaign conducted by Nash [10], who characterized the noise emitted by an octocopter delivery drone (2.5 kg payload) under realistic operating conditions, namely hovering at 10 m and 14 m above ground level, and fly over at 50 m and 16m/s. The levels presented in Table 2.1 are A-weighted sound power levels, calculated from LA_{eq} values using a procedure based on ISO 3744 [11] for the drone in hover at 10 m, covering a range of emission angles from 0° to 60° on the ground and 360° around the vehicle. The measured sound power in hover at 10 m was then used to predict flyover noise at 50 m with good agreement.

Table 2.1. A-weighted sound power of the drone

f (Hz)	L_W (dBA)	f (Hz)	L_W (dBA)
31	42.7	2000	99.1
63	71.6	4000	92.3
125	87.0	8000	81.8
250	91.9	Total:	103.3 dB(A)
500	95.2		
1000	97.9		

2.2 Environmental noise modeling

The drone's sound power was used to calibrate a free-field propagation model implemented in the iNOISE software [12], ensuring consistency with the experimental data. Deviations between measured and simulated A-weighted sound pressure levels remained within ± 0.8 dB, confirming the model's validity and its suitability for the subsequent environmental noise simulations. The urban environment considered for the simulations was a residential area in Blanchardstown, Dublin, one of the delivery drone's operational sites (Figure 2.1).

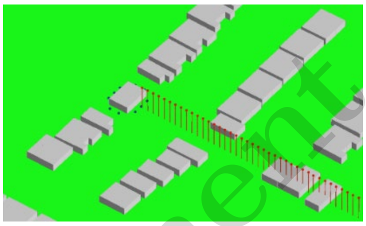

Figure 2.1. Environmental noise modeling

The ground type for the calculations was housing region, with a temperature of 20 °C, relative humidity of 60 % and wind of 5 m/s. Propagation calculations were conducted according to ISO 9613-2 [13], assuming the drone hovering at a height of 14 m above ground level and positioned 10 m horizontally from the building façade. The receiver (R) was positioned 2 m from the façade at height of 1.5 m above ground level. The results were expressed as A-weighted equivalent continuous sound pressure levels (LA_{eq}) over the 50 Hz to 5 kHz frequency range.

2.3 Glazing Samples

The sound insulation data for the glass samples were obtained from laboratory tests conducted by Scherer [14], in accordance with the ISO 10140-2:2021 [15]. Single glass systems included sealed units (1 m × 1 m) with thicknesses ranging from 4 to 8 mm, available in annealed, tempered, and laminated variants, as well as sealed double-glazed systems with air gaps of 20, 50, 100, and 150 mm. We also evaluated triple-glazed, argon-filled units (4–14–4–14–4 mm), as well as non-airtight systems, including a poorly sealed single-glazed sliding window (Sliding 1, with 4 mm glass), an improved double-glazed sliding window with enhanced sealing (Sliding 2, with 4–12–4 mm glass), and a duplicated sliding window consisting of two frames (2× Sliding 1, with 4–8.5–4 mm glass) [16].

2.4 Building Acoustic Simulations

A hypothetical bedroom (see Figure 2.2) was modeled in SONarchitect software [17] to assess whether different glazing systems could achieve the 30 dB(A) indoor acoustic comfort target [18]. The software [17] predicts the façade sound insulation ($D_{2m,nT,w}$) and the resulting indoor noise level (L_2) in the bedroom based on the ISO 12354-3:2017 standard [19]. This standard provides the engineering method specifically developed for estimating the sound insulation of façades and other external surfaces, as well as predicting indoor sound pressure levels from external noise sources. The sound source data described in Section 2.2 (R) was used as the outdoor input noise. The bedroom measures 3.3 m (façade) × 4.0 m (depth) × 3.0 m (height) and includes a brick-and-polystyrene façade (R_w = 43 dB), a blind box (R_w = 28 dB), a standard door (R_w = 29 dB), and roof and slab elements (R_w = 58 dB). In all simulations, envelope R_w values remained constant, with only the glazing system varied. Results are expressed as the received sound pressure level (L_2,dBA) and the standardized outdoor-to-indoor level difference ($D_{2m,nT,w}$, dB), according to ISO 12354-3:2017 [19].

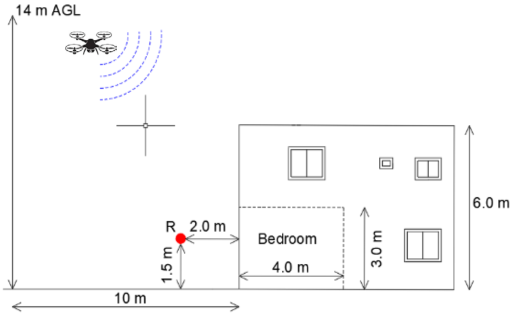

Figure 2.2. Side view of the building modelling setup

The glazing sound reduction indices used in the building acoustic simulations were measured under diffuse-field conditions according to ISO 10140 [15], whereas the numerical model assumes plane-wave incidence. Previous studies indicate that the resulting discrepancy (Plane-wave vs. ISO 10140 diffuse field) is generally limited to approximately 0–2 dB below the coincidence frequency but may increase to 3–8 dB in the coincidence region owing to the angular dependence of sound transmission. Above coincidence, typical difference is around 0–5 dB [22]. Therefore, the predicted indoor noise levels should be interpreted with this limitation in mind.

3. Results and Discussion

Figure 3.1 illustrates the average FFT of the delivery drone.

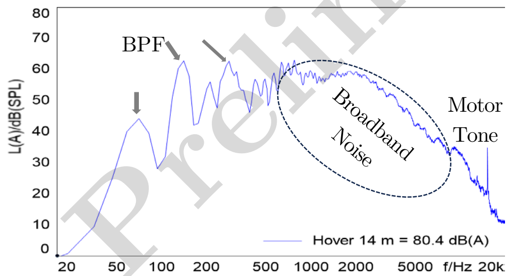

Figure 3.1. Multirotor average FFT. SPL in dB(A)

The tonal peaks observed at 70 Hz (44.3 dBA), 141 Hz (62.9 dBA), and 281 Hz (62.8 dBA) correspond to the sound pressure levels associated with the blade-passing frequency (BPF) and harmonics [20]. The spectrum further reveals two distinct regions: one dominated by broadband noise (500 Hz–10 kHz) and another characterized by a tonal peak originating from the motor's electronic speed controllers, with a level of 35 dBA at 15 kHz. While most glazing systems provide effective attenuation in the broadband noise and motor-tone regions, their performance is reduced in the BPF range. As a result, noise within this frequency band can more readily penetrate the façade, potentially leading to occupant annoyance. Accordingly, Table 3.1 summarizes the acoustic descriptors of the glazing systems analyzed, including f_c, f_0, R_w, L_2 and $D_{2m,nT,w}$. In the fifth column of Table 3.1, L_2 is the received sound pressure level in the bedroom. In the same table, (A) denotes annealed glass, (L) laminated glass, and (T) tempered glass, while the numbers 12, 20, 50, 100, and 150 represent the air cavity widths (in mm) of the double-glazed units. An overall noise level of 63.8 dB(A) was obtained at point R (2 m from the façade) from the environmental noise modelling. Among all the systems evaluated, the A4, Sliding 1, and 2× Sliding 1 configurations (marked in red in Table 3.1) failed to meet the 30 dB(A) target. The minimum required sound insulation for the glazing systems was R_w = 28 dB (Sliding 2), while the minimum composite façade insulation necessary to achieve the target was R_w = 33 dB.

Table 3.1. Resonances, Acoustic Descriptors, and Calculation Results for Glazing Systems

Glazing System	f_c (Hz	f_0 (Hz)	R_w (dB)	L_2 dB(A)	$D_{2m,nT,w}$ (dB)
A4	300	---	28	32	33
A6	250	---	29	30	34
A8	160	---	29	30	34
L6	250	---	31	29	34
L8	160	---	31	29	34
T6	250	---	29	30	34
T8	160	---	29	30	33
A4-12-A4	---	250	33	28	35
A6-20-L6	---	153	32	29	34
A6-20-L8	---	143	32	29	34
A8-20-A4	---	163	31	29	34
A8-20-A6	---	143	32	29	34
A8-20-L8	---	132	33	28	35
L6-20-L8	---	143	31	29	34
T6-20-L8	---	143	32	29	35
T8-20-L6	---	143	32	29	35
A6-50-L6	---	97	33	28	35
A6-50-L8	---	91	33	28	35
A8-50-A4	---	103	33	28	35
A8-50-A6	---	91	33	28	35
A8-50-L8	---	87	34	28	35
L6-50-L8	---	91	33	28	35
T6-50-L8	---	91	33	28	35
T8-50-L6	---	91	33	28	35
A6-100-L8	---	64	33	28	35
A8-100-A4	---	73	33	28	35
A8-100-A6	---	64	33	28	35
A8-100-L6	---	64	33	28	35
A8-100-L8	---	59	33	28	35
L6-100-L8	---	64	33	28	35
T6-100-L8	---	64	33	28	35
T8-100-L6	---	64	33	28	35

Continuation of Table 3.1:

A6-150-L6	---	56	33	28	35
A6-150-L8	---	52	34	28	35
A8-150-A4	---	59	34	28	35
A8-150-A6	---	52	34	28	35
A8-150-L8	---	48	34	28	35
L6-150-L8	---	52	33	28	35
T6-150-L8	---	52	34	28	35
T8-150-L6	---	52	34	28	35
Triple glass	---	125	34	28	35
Sliding 1	250	---	18	37	27
Sliding 2	100	---	28	30	33
2x Sliding	125	---	26	32	32

Figure 3.2 presents the L_2 spectrum (50 Hz to 5 kHz) for the bedroom equipped with 8 mm single-glazed system. Laminated glass (L8) provides more effective drone noise reduction than annealed (A8) or tempered glass (T8). In the low-frequency band (50–100 Hz), dominated by the intrusive BPF, the laminated glass achieves an average additional indoor noise reduction of up to 6.0 dB(A). At f_c (1600 Hz), it further outperforms the other glass types, achieving an additional 4.2 dB(A) of attenuation. This superior performance is attributable to laminated glass's inherently higher loss factor and enhanced damping characteristics.

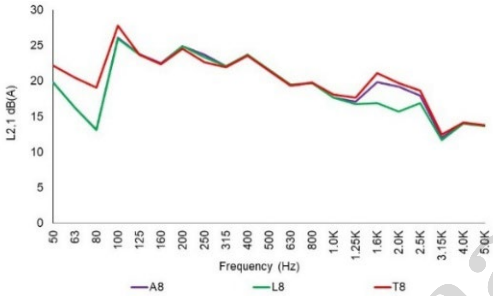

Figure 3.2. L_2 spectrum in dB(A) for 8 mm single glass

Figure 3.3 illustrates the influence of air gap width on drone noise reduction for double-glazed units.

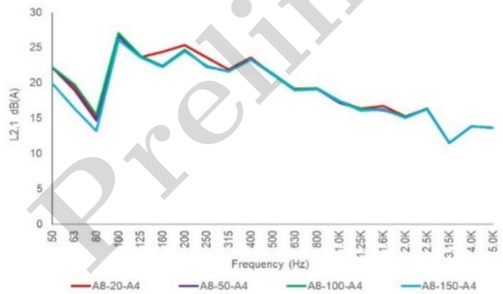

Figure 3.3. L_2 spectrum in dB(A) for double-glazed units

Increasing the air gap in double-glazed systems from 20 mm to 150 mm reduces drone noise in the 50–100 Hz range by up to 3.1 dB(A), with the maximum reduction occurring at 63 Hz. Another effect is the downward shift of f_0, decreasing from 163 Hz (20 mm air gap) to 103 Hz (50 mm), 73 Hz (100 mm), and 59 Hz (150 mm).

Ramos-Romero et al. [21] report that drone flyover spectra depend on size: larger drones mainly generate broadband noise, while smaller ones show stronger tonal components. Therefore, glazing selection and building regulations should consider drone weight category to address the dominant acoustic component. Figure 3.4 compares the indoor attenuation of drone noise for L8, Sliding 1, Sliding 2, 2 × Sliding 1, and the argon-filled triple-glazed unit.

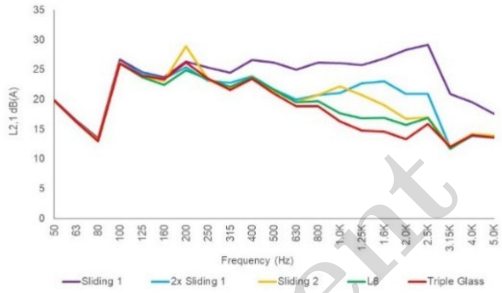

Figure 3.4. L_2 spectrum in dB(A) for Triple-glazed, Sliding 1, 2 x Sliding 1, Sliding 2 and L8 glass system

The low airtightness of Sliding 1 does not sufficiently attenuate the tonal or broadband components of drone noise, producing a high indoor level of 37 dB(A), unsuitable for rest. Adding a second identical Sliding 1 window provides a 5 dB(A) overall reduction, with improvement from 200 Hz to 5 kHz. However, it still does not match the insulation performance of a single 8 mm laminated glass. The results for the double-glazed sliding window with improved airtightness (Sliding 2) confirm that, under drone noise conditions, acoustic performance is governed by airtightness rather than the glass configuration. This is illustrated in Figure 3.5, which compares indoor drone noise levels for Casement and Sliding 2 windows, both fitted with the same double-glazed unit (4 mm–12 mm air gap–4 mm).

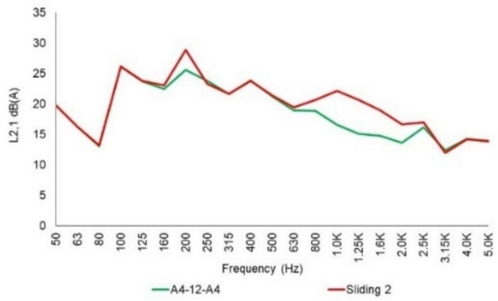

Figure 3.5. L_2 spectrum in dB(A) for casement window (A4-12-A4) and Sliding window 2

While the Sliding 2 window (a common typology in Mediterranean Europe) yields an overall indoor drone noise of 30 dB(A) with a 200 Hz peak of 28.9 dB(A), a better-sealed alternative reduces this peak by 3.3 dB(A) and lowers the indoor overall level from 30 dB(A) to 28 dB(A). This improvement spans a wide frequency range, with gains reaching 5.6 dB(A) from 630 Hz to 2.5 kHz. Most of the glazing systems evaluated in this study were able to meet the indoor acoustic comfort target (see Table 3.1). However, given the disruptive nature of drone noise and its broadband emission across nearly the entire audible frequency range, the inadequacy of single-number metrics for characterizing drone noise becomes evident. For instance, as shown in Figure 3.3, both the A8-50-A4 and A8-150-A4 double-glazed systems achieve the same overall indoor noise level of 28 dB(A). Yet, the system with the larger interlayer spacing exhibits superior low-frequency performance and shifts f_0 below 59 Hz. Consequently, regulatory frameworks and building codes must move beyond single-number ratings to incorporate frequency-specific criteria that address the unique acoustic signature of drone noise, thereby ensuring true indoor acoustic comfort. Supplementary façade simulations, without the blind box, showed a reduction of 0 – 2 dB for less airtight glazing systems (i.e., Sliding 1, Sliding 2, and 2x Sliding 1), compared to 1 – 3 dB for single-glazed systems, and 3 – 4 dB for double-glazed systems. Figure 3.6 illustrates the internal noise level of the drone within the assessed bedroom, for a casement window with double glazing (4-12-4 mm), with and without the presence of the blind box. A noise reduction can be observed across the entire spectrum. At low frequencies, between 50 and 500 Hz, this reduction is more moderate, with 2.2 dB(A) at 125 Hz and 250 Hz. On the other hand, in the mid and high-frequency range, a significant noise reduction is observed for the window without the blind box, reaching 9.6 dB(A) less at 4 kHz. Thus, the presence or absence of a blind box on the façade will have a greater impact on the transmission of broadband noise and motor tones from the drone.

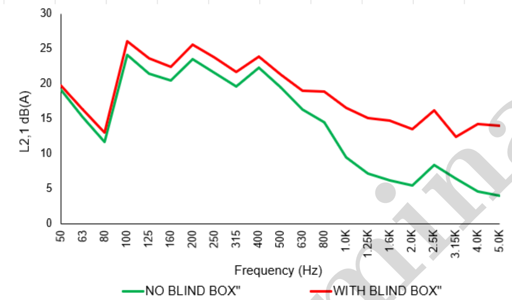

Figure 3.6. L_2 spectrum in dB(A) for casement window (A4-12-A4) with and without blind box

3.1 Limitations

The study is subject to some limitations. It uses a single 2.5 kg drone acoustic profile recorded during hover at 14 m altitude, without accounting for variations in drone type, payload, or flight maneuvers. Indoor levels were predicted using simulations without in-situ validation, for a single bedroom configuration and façade system. Thus, results may differ across architectural settings and should be regarded as estimates. Finally, economic aspects of high-performance solutions, such as triple glazing, were beyond the study scope.

4. Conclusions

This study evaluated the potential of different glazing systems to mitigate indoor noise from delivery drones and to meet recommended thresholds of acoustic comfort, yielding performance-based guidelines for façade design in response to this emerging urban noise source. The results indicate that, for single-glazed systems, laminated glass consistently outperforms annealed and tempered glass of equivalent thickness due to its superior damping characteristics, yielding an average additional indoor noise reduction of 6.0 dB(A) in the low-frequency range (50–100 Hz) dominated by the blade-passing frequency, as well as an extra reduction of about 4.2 dB(A) at the critical frequency (1600 Hz). Among the single-glazing systems studied, the minimum thickness required to achieve the acoustic comfort threshold was 6 mm. For double-glazed systems, acoustic performance is largely governed by f_0. Increasing the air cavity width from a conventional 12 mm to 100 or 150 mm substantially improves low-frequency attenuation. This increase shifts f_0 downward, from 250 Hz to 48 Hz in the analysed cases, effectively decoupling the system resonance from the dominant tonal components of drone noise and reducing sound levels in the 50–100 Hz band by up to 3.1 dB(A). Furthermore, the analysis of window typologies demonstrates that airtightness is often more critical to overall acoustic performance than the glazing unit itself. For instance, a poorly sealed sliding window produced indoor noise level peaks of 28.9 dB(A) at 200 Hz, whereas a well-sealed casement window with identical double glazing reduced this peak by 3.3 dB(A) and provided broadband improvements of up to 5.6 dB(A). The study also shows that single-number ratings such as R_w are insufficient to characterize glazing performance against drone noise, as different systems may result in the same overall indoor level while exhibiting markedly different frequency-dependent attenuation, particularly in the low-frequency range where drone noise is most intrusive. Overall, effective glazing design for drone noise mitigation requires a frequency-specific approach that prioritizes high-damping materials such as laminated glass for single panes, maximizes cavity width in double-glazed units to lower f_0, and ensures excellent perimeter sealing. The study is a practical framework for designers and policymakers to safeguard indoor acoustic comfort in urban environments increasingly exposed to drone activity. Future work should complement the present findings with perceptual evaluations, such as psychoacoustic listening tests with building occupants, to relate objective acoustic metrics to subjective responses including annoyance and perceived loudness. In addition, comparative assessments of glazing performance under different drone operating modes, such as variations in flight speed, altitude, or manoeuvring conditions, would help establish the robustness of these systems under a broader range of real-world operational noise scenarios.

5. Acknowledgments

This work was financially supported by the HEAD–Genuit Foundation (Project number: P-24/07-W). The authors also gratefully acknowledge the institutional support provided by the Faculty of Science, Technology, Engineering and Mathematics (STEM) at Trinity College Dublin.

References

[1] Torresin, S., Aletta, F., Dicle, S., Albatici, R., de Dear, R., Hasegawa, Y., Kang, J., Parkinson, T., & Cabrera, D. (2024). Towards developing a model of adaptive acoustic comfort in the built environment: A thematic analysis from an expert focus group. Building and Environment, 266. https://doi.org/10.1016/j.buildenv.2024.112074 A. Someone, B. Someone, and C. Someone: "The title of the journal paper," *Journal of Name*, vol. A, no. B, pp. 111–222, 2010.

[2] Berardi, U., Ivona, C., & Stasi, R. (2025). Sound insulation improvements in lift-and-slide window systems. Building and Environment, 282. https://doi.org/10.1016/j.buildenv.2025.113258.

[3] Patrício, J. (2020). Acústica nos edifícios (7th ed. rev. and enl.). Verlag Dashöfer

[4] Arenas, J. P. (2025). On the impact of electric vehicle transition on urban noise pollution. In Current Opinion in Environmental Science and Health (Vol. 45). Elsevier B.V. https://doi.org/10.1016/j.coesh.2025.100623

[5] Straubinger, A., Verhoef, E. T., & de Groot, H. L. F. (2022). Going electric: Environmental and welfare impacts of urban ground and air transport. Transportation Research Part D: Transport and Environment, 102. https://doi.org/10.1016/j.trd.2021.103146

[6] Casagrande Hirono, F., Robertson, J., & Torija Martinez, A. J. (2024). Acoustic and psychoacoustic characterization of small-scale contra-rotating propellers. Journal of Sound and Vibration, 569. https://doi.org/10.1016/j.jsv.2023.117971

[7] Lee, S. M., Wie, S. Y., & Haan, C. H. (2025). Noise Modeling of Urban Vertiport Areas Depending on the K-UAM Operation. International Journal of Aeronautical and Space Sciences, 26(5), 2968–2983. https://doi.org/10.1007/s42405-025-00932-8

[8] Ramos-Romero, C., Green, N., Roberts, S., Clark, C., & Torija, A. J. (2022). Requirements for Drone Operations to Minimize Community Noise Impact. International Journal of Environmental Research and Public Health, 19(15). https://doi.org/10.3390/ijerph19159299

[9] Masullo, M., Gravina, N., Iaderosa, R., Zerlenga, O., & Maffei, L. (n.d.). An investigation on the effects of drone noise in an urban context Session: Human Response to Urban Air Mobility (UAM) Noise.

[10] Nash, A., & Kennedy, J. (2024, September 8-11). In flight evaluation of UAV noise emission. QUIETDRONES 2024, Manchester.

[11] International Organization for Standardization. (2010). Acoustics — Determination of sound power levels and sound energy levels of noise sources using sound pressure — Engineering methods for an essentially free field over a reflecting plane (ISO Standard No. 3744:2010). https://www.iso.org/standard/52009.html

[12] Inoise. https://inoise.com. (Accessed 10 February 2026) [Online].

[13] International Organization for Standardization. (1996). Acoustics — Attenuation of sound during propagation outdoors — Part 2: General method of calculation (ISO 9613-2:1996). (ISO Standard No. 9613-2).

[14] Scherer, M. J. (2005). Sound insulation study of glass of different types and thicknesses in single and double glazing (Master's dissertation). Federal University of Santa Maria, Graduate Program in Civil Engineering, Santa Maria, RS, Brazil.

[15] International Organization for Standardization. (2021). ISO 10140-2:2021 — Acoustics — Laboratory measurement of sound insulation of building elements — Part 2: Measurement of airborne sound insulation. ISO.

[16] Oliveira, M. A. (2007). Estudo da eficiência da duplicação de janelas na melhoria do isolamento acústico destes componentes [Master's dissertation, Federal University of Santa Maria]. Digital Library of Theses and Dissertations of UFSM

[17] SONarchitect.https://www.soundofnumbers.net/sonarchitect/index.php/en/. (Accessed 1 January 2026) [Online].

[18] World Health Organization. (1999). Guidelines for community noise. (B. Berglund, T. Lindvall, & D. H. Schwela, Eds.). https://iris.who.int/handle/10665/66217

[19] International Organization for Standardization. (2017). Acoustics - Building acoustics - Part 3: Transmission of sound through building elements (ISO 12354-3:2017). https://www.iso.org/standard/66261.html

[20] Sarikaya, B., Zarri, A., Christophe, J., Aissa, M. H., Verstraete, T., & Schram, C. (2024). Aerodynamic and aeroacoustic design optimization of UAVs using a surrogate model. Journal of Sound and Vibration, 589. https://doi.org/10.1016/j.jsv.2024.118539

[21] Ramos-Romero, C., Green, N., Torija, A. J., & Asensio, C. (2023). On-field noise measurements and acoustic characterisation of multi-rotor small unmanned aerial systems. Aerospace Science and Technology, 141. https://doi.org/10.1016/j.ast.2023.108537

[22] Craik, R. J. M. (1996). Sound transmission through buildings. Taylor & Francis.